HTML ABSTRACT + LINKS

Interface structure and non-stoichiometry in HfO_2 dielectrics

Hion Suck Baik, Miyoung Kim, Gyeong-Su Park, and Se Ahn Song
Analytical Engineering Center, Samsung Advanced Institute of Technology, P. O. Box 111, Suwon 440-600, Korea

Maria Varela
Condensed Matter Sciences Division, Oak Ridge National Laboratory, P. O. Box 2008, Oak Ridge, Tennessee 37831-6030

A. Franceschetti and S. T. Pantelides
Department of Physics, Vanderbilt University, Nashville, Tennessee 37064 and Condensed Matter Sciences Division, Oak Ridge National Laboratory, P. O. Box 2008, Oak Ridge, Tennessee 37831-6030

S. J. Pennycook[a)]
Condensed Matter Sciences Division, Oak Ridge National Laboratory, P. O. Box 2008, Oak Ridge, Tennessee 37831-6030 and Department of Physics, Vanderbilt University, Nashville, Tennessee 37064

(Received 23 February 2004; accepted 18 May 2004)

High-resolution electron microscopy, electron energy-loss spectroscopy, and first-principles theory are used to investigate the composition and electronic structure of HfO_2 dielectric layers deposited directly onto Si. A thin, nonstoichiometric, but Hf-free SiO_2 layer forms between the HfO_2 dielectric and the substrate, consistent with one-dimensional spinodal decomposition. Rapid thermal annealing crystallizes the HfO_2, and the resulting grain boundaries within the HfO_2 are found to be O-depleted, with localized states within the bandgap. These localized states are thought to act as significant leakage pathways, and may be responsible for Fermi-level pinning at the dielectric/contact interface. © *2004 American Institute of Physics*. [DOI: 10.1063/1.1772855]

HfO_2 dielectrics have been studied extensively for future gate oxides and capacitors due to their high dielectric constant, relatively large bandgap, and good thermal stability with Si.[1,2] The formation of silicates is generally thought to be kinetically suppressed. Amorphous Hf-Si-O separates into HfO_2- and SiO_2-like regions via spinodal decomposition or by nucleation and growth of HfO_2 precipitates, depending on whether the composition lies outside the miscibility gap or not.[3–7] Generally, the device structure involves a compromise between maintaining sufficiently *low* Hf concentration that the dielectric remains amorphous during processing, and is therefore of high electrical quality, and achieving a sufficiently *high* Hf content to give a low SiO_2 equivalent thickness. Numerous studies have addressed these issues, but the conclusions are often conflicting.[8–16]

In this letter, we combine high-resolution transmission electron microscopy (HRTEM), scanning transmission electron microscopy (STEM), electron energy-loss spectroscopy (EELS), and calculations based on density functional theory to explore the nature and properties of these interfaces. A number of dielectric and interface structures were fabricated, and a thin, Hf-free, SiO_2 layer was found to have formed at the Si interface. As reported for Zr-silicate films, such an interface may allow good interface passivation to be achieved and high gate channel mobilities.[17] Our samples were fabricated using pure HfO_2 films deposited directly onto Si, and as expected, were crystallized on rapid thermal annealing (RTA). The resulting grain boundaries were found to be oxygen deficient with localized states within the bandgap. We believe these states may be responsible for the high leakage currents in these devices and may also represent the traps responsible for Fermi-level pinning.

Four different TiN (100 Å)/HfO_2 (50 Å)/Si types of films were prepared for this study. In all cases, Si substrates were first cleaned with a NH_4OH/H_2O_2 solution, and HfO_2 films were then deposited by the atomic layer deposition (ALD) method using tetrakis(ethylmethylamido)hafnium with 48 cycles at 300 °C. Next, a 100 Å TiN electrode was deposited either by ALD or by chemical vapor deposition (CVD) using a $TiCl_4/NH_4$ precursor in both cases. The TiN deposition temperature for ALD was 450 °C and for CVD was 600 °C. In both cases, the HfO_2 crystallized during the deposition. We will refer to these samples as ALD and CVD, respectively. Another two sets of samples were prepared in the same way, except that the HfO_2 layers were first given a RTA for 120 s at 750 °C in a N_2 atmosphere. The dielectric films crystallized during the RTA. We will refer to these samples as CVD RTA and ALD RTA.

HRTEM images of the four samples are shown in Fig. 1, obtained using a FEI F30 UT equipped with a Gatan ENFINA system at Samsung (point resolution 1.4 Å, STEM probe ~3 Å). Table I compares the thickness of the interfacial layer and the dielectric film in each case. In the ALD sample, the interfacial layer between the Si substrate and HfO_2 film increased by 3 Å during the RTA and the HfO_2 layer thickness increased by the same amount. These observations suggest that the oxygen responsible for the increased thickness did not originate from the specimen, but from the ambient atmosphere during the RTA. A similar effect has been noted by Stemmer *et al.*[18] during the N_2 processing of hafnium aluminate dielectrics. The higher processing temperature during CVD resulted in a thicker initial interfacial layer, which again increased by 3 Å during the RTA. The thickness of the as-deposited CVD dielectric layer appears to be significantly smaller than the ALD layer.

[a)]Electronic mail: pennycooksj@ornl.gov

 © 2004 American Institute of Physics
Downloaded 25 Oct 2004 to 160.91.49.10. Redistribution subject to AIP license or copyright, see http://apl.aip.org/apl/copyright.jsp

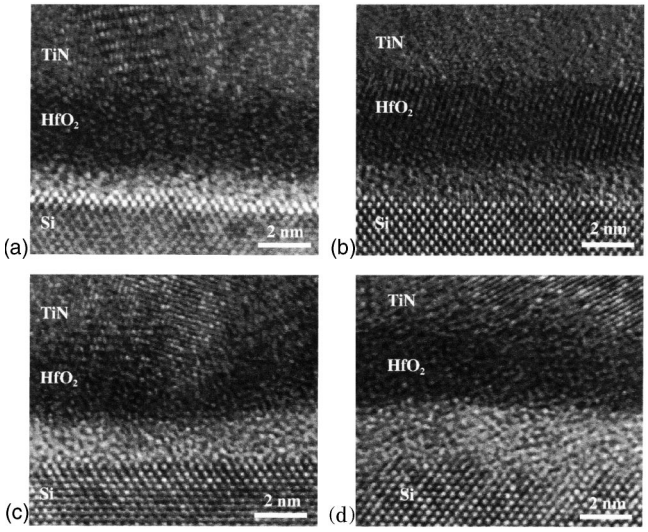

FIG. 1. HRTEM images of the samples (a) TiN grown by ALD on as-deposited HfO_2, (b) TiN grown by ALD on RTA HfO_2, (c) TiN grown by CVD on as-deposited HfO_2, (d) TiN grown by CVD on RTA HfO_2.

A *Z*-contrast image of one of the four samples is shown in Fig. 2, obtained with a VG Microscopes HB603 STEM equipped with Nion aberration corrector. The probe size on the instrument is below 1 Å.[19] Since the intensity in *Z*-contrast images is roughly proportional to atomic number (*Z*) squared, they are dominated by the presence of Hf ($Z=72$). All samples showed similar features. The intensity trace clearly delineates the Hf concentration profile and allows the widths of the interfacial and dielectric layers to be accurately determined, as given in Table I. They differ quite significantly from the values obtained from the phase contrast images, which highlights the fact that the phase contrast and *Z*-contrast images exhibit different sensitivities to structure and composition, as discussed recently by Diebold *et al.*[20] The phase contrast image is primarily sensitive to crystallinity; sensitivity to Hf is based on absorptive contrast, which is secondary. The estimated dielectric thickness of the CVD sample from Fig. 1(c) is smaller than that obtained from the *Z*-contrast image in Fig. 2 because of some etching of the HfO_2 during CVD deposition of TiN. The strong TiN lattice fringes tend to mask the dark band of the Hf layer leading to an underestimate of the Hf layer thickness. In the *Z*-contrast image, the Hf dominates and the actual layer thickness is clear.

Similarly, the interfacial layer thicknesses estimated from the two techniques also differ. With the *Z*-contrast image, the thickness was obtained using a number of profiles each averaged over a 4 nm length of interface, and was defined as the separation between the two points showing intensity midway between that of Si and that of the SiO_2 layer. The increase in thickness of the interfacial layer in the CVD case is less than estimated from the phase contrast image. *Z*-contrast images also provide a reliable measure of interface roughness.[20] In all samples, the interfacial roughness between the Si and the interfacial layer is ~4 Å.

TABLE I. Thickness of interfacial and dielectric layers by TEM and STEM. Error estimates are for statistical errors only.

	Interfacial layer (TEM) (Å)	Interfacial layer (STEM) (Å)	Dielectric layer (TEM) (Å)	Dielectric layer (STEM) (Å)
ALD as-deposited	10 (±1)	8 (±1)	34 (±2)	30 (±1)
ALD after RTA	14 (±1)	10 (±1)	38 (±3)	31 (±1)
CVD as-deposited	15 (±1)	13 (±1)	21 (±1)	33 (±1)
CVD after RTA	20 (±1)	15 (±1)	33 (±2)	34 (±2)

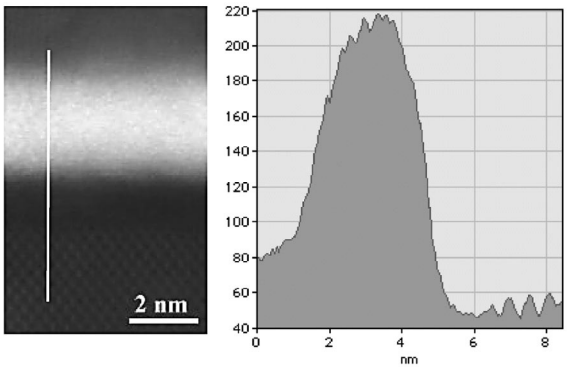

FIG. 2. High-resolution *Z*-contrast image of TiN grown by CVD on as-deposited HfO_2 with intensity trace along the [100] direction, marked in white, showing the HfO_2 layer (high intensity), the SiO_2 layer and the first few dumbbells of the Si lattice.

The right-hand side of the intensity profile in Fig. 2 covers the first few Si atomic columns of the substrate and shows the 0.54 nm periodicity along the [100] direction. The traces confirm that there is minimal Hf at the Si/SiO_2 interface. This observation is consistent with the one-dimensional spinodal decomposition predicted by Kim *et al.*[14] It may therefore be possible to passivate this interface to achieve high gate mobilities.

The lack of significant Hf in the interfacial layer is confirmed by the low loss EELS data shown in Fig. 3(a), containing the Hf O_{23} edge. Data was obtained using a VG Microscopes HB501UX dedicated (STEM at ORNL probe ~1.3 Å) equipped with Nion aberration corrector and a PEELS system. The Hf peak is clearly absent from the SiO_2 interfacial layer. To investigate the electronic properties of the interfacial SiO_2 layer. O K EELS profiles were also collected. Figure 3(b) shows results for several locations between the Si/SiO_2 interface to the center of the dielectric layer for the case of the CVD-RTA sample. The O K edge within the dielectric layer shows the characteristic double peak structure of HfO_2.[18] As also noted by Stemmer *et al.*,[18] this double peak structure was present in both the RTA and the uncrystallized samples. Moving into the interfacial layer, there is a progressive decrease in the initial peak until it disappears in the amorphous interfacial layer. Within the

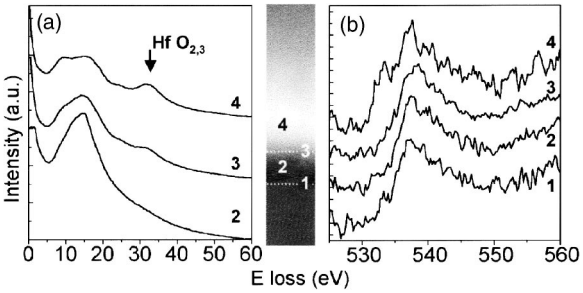

FIG. 3. (a) Low loss EELS results using a 1.3 Å probe for the CVD RTA sample. The Hf $O_{2,3}$ edge at 31 eV is marked with an arrow. (b) O-K EELS results for the CVD sample.

Downloaded 25 Oct 2004 to 160.91.49.10. Redistribution subject to AIP license or copyright, see http://apl.aip.org/apl/copyright.jsp

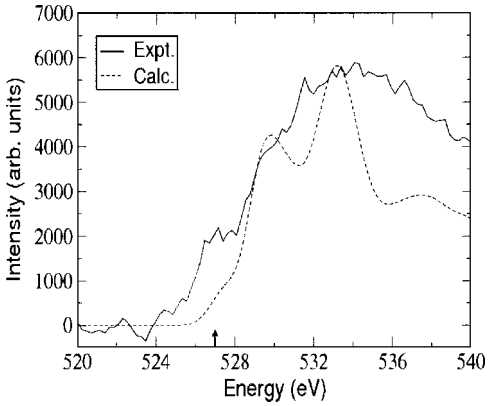

FIG. 4. EELS from a grain boundary (solid line) showing a prepeak at ~527 eV (upward arrow). The splitting of the two HfO_2 peaks is also reduced compared to the bulk (Fig. 3 spectrum 4). The calculated EELS spectrum (dotted line) from an O atom in HfO_2 next to an O vacancy also has a shoulder at ~527 eV.

SiO_2 layer we find a small shoulder in the near edge structure, which is indicative of states in the bandgap. As Hf is absent from this region, this indicates that the oxide is nonstoichiometric. The prepeak increases further at the Si/SiO_2 interface, as typically found for such interfaces due to the presence of suboxide bonding.[21,22]

Capacitors were prepared using a poly-Si bottom electrode, nitridation by RTA in NH_3, depositing a HfO_2 dielectric layer by ALD, followed by a TiN top electrode and poly-Si cap. Unfortunately, these samples had a leakage current too high for electrical characteristics to be collected. Presumably this is due to the polycrystalline nature of the HfO_2 dielectric. Prior work in $SrTiO_3$ grain boundaries[23] has already shown the presence of grain boundary states due to nonstoichiometry. Therefore, we examined the EEL spectra from a grain boundary in the dielectric layer to investigate the possibility of additional states that might act as leakage pathways. Spectra from the boundary indeed show a prepeak in the near edge fine structure, suggesting the presence of interface states, as shown in Fig. 4.

To test whether the origin of this prepeak is due to nonstoichiometry effects, such as the presence of oxygen vacancies, first-principles calculations were performed using density-functional theory in the generalized-gradient approximation. An O vacancy was introduced in a large, 96-atom HfO_2 supercell (monoclinic phase), and the atoms around the vacancy were allowed to relax. The O vacancy gives rise to localized electronic states near the conduction-band edge, which have significant weight only on the Hf and O atoms directly surrounding the vacancy. The O K spectrum was calculated using the $Z+1$ approximation.[24] The presence of O vacancies resulted in a shoulder in the K edge of neighboring O atoms (arrowed in Fig. 4), in the same position as the prepeak seen in the EEL spectrum from the grain boundary. Our results therefore indicate that oxygen vacancies at the grain boundaries introduce interface states, possibly explaining the Fermi-level pinning effects reported recently[16] and the high leakage. Other workers, however, have reported that crystallization of the HfO_2 does not increase leakage current.[14] Further work is required to investigate the nature of grain boundaries in HfO_2.

This work was supported by National Laboratory program (Grant No. 2000-N-NL-C-205). We gratefully acknowledge J.H. Yeo and J.H. Oh (Process Development Team, Samsung Electronics Co., Ltd.) for providing the samples. This research was supported in part by Oak Ridge National Laboratory, managed by UT-Battelle, LLC, for the U.S. Department of Energy under Contract No. DE-AC05-00OR22725, by the Air Force Office of Scientific Research MURI Grant F-49620-99-1-0289, and by the McMinn Endowment at Vanderbilt University. Research of one of the authors (M.V.) is performed as a Eugene P. Wigner Fellow and staff member at ORNL.

[1] L. Kang, Y. Jeon,K. Onishi, B. H. Lee, W.-J. Qi, R. Nieh, S. Gopalan, and J. C. Lee, presented at the *2000 Symposium on VLSI Technology, Digest of Technical Papers, Honolulu, HA, June 15–17* (Institute of Electrical and Electronics Engineers, Piscataway, NJ, 2000).
[2] M. Balog, M. Schieber, M. Michiman, and S. Patai, Thin Solid Films **41**, 247 (1977).
[3] M. H. Cho, Y. S. Roh, C. N. Whang, K. Jeong, S. W. Nahm, D. H. Ko, J. H. Lee, N. I. Lee, and K. Fujihara, Appl. Phys. Lett. **81**, 472 (2002).
[4] J. Morais, L. Miotti, G. V. Soares, S. R. Teixeira, R. Pezzi, K. P. Bastos, I. J. R. Baumvol, A. L. P. Rotondaro, J. J. Chambers, M. R. Visokay, and L. Colombo, Appl. Phys. Lett. **81**, 2995 (2002).
[5] H. Kim and P. C. McIntyre, J. Appl. Phys. **92**, 5094 (2002).
[6] P. S. Lysaght, B. Foran, G. Bersuker, P. J. J. Chen, R. W. Murto, and H. R. Huff, Appl. Phys. Lett. **82**, 1266 (2003).
[7] S. Stemmer, Y. L. Li, B. Foran, P. S. Lysaght, S. K. Streiffer, P. Fuoss, and S. Seifert, Appl. Phys. Lett. **83**, 3141 (2003).
[8] J. Aarik, A. Aidla, A.-A. Kiisler, T. Uustare, and V. Sammelselg, Thin Solid Films **340**, 110 (1999).
[9] S. Sayan, S. Aravamudhan, B. W. Busch, W. H. Schulte, F. Cosandey, G. D. Wilk, T. Gustafsson, and E. Garfunkel, J. Vac. Sci. Technol. A **20**, 507 (2002).
[10] M. Cho, J. Park, H. B. Park, C. S. Hwang, J. Jeong, and K. S. Hyun, Appl. Phys. Lett. **81**, 334 (2002).
[11] B. H. Lee, L. Kang, R. Nieh, W.-J. Qi, and J. C. Lee, Appl. Phys. Lett. **76**, 1926 (2000).
[12] K. Kukli, M. Ritala, J. Sundqvist, J. Aarik, J. Lu, T. Sajavaara, M. Leskela, and A. Harsta, J. Appl. Phys. **92**, 5698 (2002).
[13] K. Saito, Y. Jin, and M. Shimada, Appl. Phys. Lett. **81**, 3582 (2002).
[14] H. Kim, P. C. McIntyre, and K. C. Saraswat, Appl. Phys. Lett. **82**, 106 (2003).
[15] J. K. Schaeffer, S. B. Samavedam, D. C. Gilmer, V. Dhandapani, P. J. Tobin, J. Mogab, B.-Y. Nguyen, B. E. White Jr., S. Dakshina-Murthy, R. S. Rai, Z.-X. Jiang, R. Martin, M. V. Raymond, M. Zavala, L. B. La, J. A. Smith, R. Garcia, D. Roan, M. Kottke, and R. B. Gregory, J. Vac. Sci. Technol. B **21**, 11 (2003).
[16] C. Hobbs, L. Fonseca, V. Dhandapam, S. Sarnavedarn, B. Taylor, J. Grant, L. Dip, D. Triyoso, R. Hegde, D. Gilmer, R. Garcia, D. Roan, L. Lovejoy, R. Rai, L. Hebert, H. Tseng, B. White, and P. Tobin, presented at the *2003 Symposium on VLSI Technology, Digest of Technical Papers*, Honolulu, HA, June 12–14 (Institute of Electrical and Electronics Engineers, Piscataway, NJ, 2003).
[17] D. A. Muller and G. D. Wilk, Appl. Phys. Lett. **79**, 4195 (2001).
[18] S. Stemmer, Z. Q. Chen, W. J. Zhu, and T. P. Ma, J. Microsc. **210**, 74 (2003).
[19] S. J. Pennycook, A. R. Lupini, M. Varela, A. Borisevich, M. F. Chisholm, E. Abe, N. Dellby, O. L. Krivanek, P. D. Nellist, L. G. Wang, R. Buczko, X. Fan, and S. T. Pantelides, in *Spatially Resolved Characterization of Local Phenomena in Materials and Nanostructures*, edited by D. A. Bonnell, A. J. Piqueras, P. Shreve, and F. Zypman (Materials Research Society, Warrendale, Pennsylvania, 2003), p. G1.1.
[20] A. C. Diebold, B. Foran, C. Kisielowski, D. A. Muller, S. J. Pennycook, E. Principe, and S. Stemmer, Microsc. Microanal. **9**, 493 (2003).
[21] D. A. Muller, T. Sorsch, S. Moccio, F. H. Baumann, K. Evans-Lutterodt, and G. Timp, Nature (London) **399**, 758 (1999).
[22] S. T. Pantelides, M. Ramamoorthy, S. Rashkeev, R. Buczko, G. Duscher, and S. J. Pennycook, in *Fundamental Aspects of Silicon Oxidation*, edited by Y. J. Chabal (Springer, Berlin, 2001), p. 193.
[23] M. Kim, G. Duscher, N. D. Browning, S. J. Pennycook, K. Sohlberg, and S. T. Pantelides, Phys. Rev. Lett. **86**, 4056 (2001).
[24] B. Johansson and N. Martensson, Phys. Rev. B **21**, 4427 (1980).

Downloaded 25 Oct 2004 to 160.91.49.10. Redistribution subject to AIP license or copyright, see http://apl.aip.org/apl/copyright.jsp